

SMASIS2013-3063

TESTING OF VIBRATIONAL ENERGY HARVESTING ON FLYING BIRDS

Michael W. Shafer *

Sibley School of Mechanical
and Aerospace Engineering
Cornell University
Ithaca, New York 14853
Email: mws228@cornell.edu

Robert MacCurdy

Sibley School of Mechanical
and Aerospace Engineering,
Cornell University
Ithaca, New York 14853
Email: rbm7@cornell.edu

Ephraim Garcia

Sibley School of Mechanical
and Aerospace Engineering
Cornell University
Ithaca, New York 14853
Email: eg84@cornell.edu

ABSTRACT

Discrete animal-mounted sensors and tags have a wide range of potential applications for researching wild animals and their environments. The devices could be used to monitor location, metabolic output, or used as environmental monitoring sentinels. These applications are made possible by recent decreases in the size, mass, and power consumption of modern microelectronics. Despite these performance increases, for extended deployments these systems need to generate power in-situ. In this work, we explore a device that was recently deployed to test the concept of piezoelectric energy harvesting on flying birds. We explain the development of the device and introduce test results conducted on flying pigeons (*Columba livia*). The testing device consisted of a miniature data acquisition system, piezoelectric energy harvester, and actuator system. The output of the energy harvester was monitored by a microcontroller and recorded throughout the flight. The energy harvester included a wireless receiver, battery and linear servo. By remotely actuating the linear servo, we were able to arrest the energy harvester for portions of the flight. In doing so, we will be able to compare flight accelerations of a bird with a simple proof mass and with a dynamic mass without having to stop the flight of the bird. The comparison of these two cases allows for the assessment of the feasibility of employing vibrational energy harvesting on a flying bird. We present the initial results of this testing with regard to the harvested power and the in-flight acceleration profiles.

Keywords: *energy harvesting, avian, bird, piezoelectric, testing*

Introduction

The direct study of animals in their natural environment through observation can be challenging or impossible for many species. "Bio-logging" devices are systems mounted to an animal used to record data about the host or its environment without the need for direct observations by a human [1]. Owing their names to "biology" and "data-logging," these devices can drastically increase amount of data available to scientists interested in animals and their habitats. Modern bio-logging devices are often composed of a suite of sensors run by a microcontroller, and typically powered by a battery. Fundamentally, the science that can be conducted directly depends on the power budget of the system, and thus is limited by battery technology. In this work we consider how vibrational energy harvesting could be used to supplement the power budget of bio-logging devices. Specifically, we focus on a device developed to conduct tests of piezoelectric energy harvesters on flying rock pigeons (*Columba livia*) and show that a significant amount of power can be harvested in flight from these birds.

The concept of animal-based data collection can be traced back to a depth recording device placed on a harpooned fin whale (*Balaenoptera physalus*) in the 1930's [2] and Weddell seals (*Leptonychotes weddellii*) in the 1960's [3]. In the time since their initial deployment, bio-logging devices have seen drastic improvements in capabilities, both in terms of the number of sensors and the resolution and frequency of measurements [4] [5]. In large part, these increases in capabilities have been a result of reductions in the power consumption of modern microelectronic

*Address all correspondence to this author.

components. Modern systems are capable of measuring anything from position to acoustics, but are still fundamentally limited to the amount of energy stored in their batteries [6] [7]. If power could be generated throughout the life of the tag, smaller batteries could be used and more energy intensive sensors could be deployed.

Vibrational energy harvesting on living animals has been demonstrated previously on moths (*Manduca sexta*) and green june beetles (*Cotinis nitida*) [8] [9]. Additionally, we have previously shown that there is a significant amount of power available for harvest from the flight of the majority of birds, even after accounting for the power required to carry the system [10]. In this work we review the testing conducted to measure the harvested power on a bird, and describe in detail the device developed to measure the harvester power and acceleration on the birds in flight. We also present some typical results from the more than 120 trials to show that there is a significant amount of power that can be harvested.

1 Testing Overview

In order to address the feasibility of harvesting vibrational energy on flying birds, we had two primary objectives in testing: (1) Understand the effects of a dynamic mass on the flight of a bird. (2) Measure the power harvested by a piezoelectric device in flight. While it is known that birds can generally carry up to 2-4% of their body mass without considerable effects on long-term survivability, these numbers are based on a static mass [11] [12] [13] [14]. In order to determine if piezoelectric energy harvesting is viable on a flying bird, we must determine if a vibrating system would adversely affect a bird's flight capabilities. To measure any effect, we developed a system that was able to measure the accelerations of the bird in flight with a piezoelectric beam that could be remotely locked down or allowed to vibrate. This allowed for a series of tests with and without a vibrating element on the back of the bird.

The test was designed to measure any effect of the vibrating system and consisted of flying a bird back and forth between two perches in a room while measuring the acceleration and harvested power. The test began by attaching a small energy harvester and data acquisition system (DAQ) to the back of three rock pigeons (*Columba livia*). After turning on the on-bird DAQ, each pigeon was then placed in a room with only two perches spaced 22 ft. apart, between which they had previously been trained to fly. The energy harvester was then locked down, so as not to vibrate and the bird was prompted to fly from one perch to the other. The bird was then prompted to fly back to the original perch. Remotely, the energy harvesting beam was then released and allowed to vibrate. The bird was prompted to fly back and forth between the perches again. This process of flying between perches and locking/releasing the harvester device was then repeated multiple times.

The device that was attached to the bird consisted of three integrated subsystems: the piezoelectric energy harvester device, the data-logging system, and the beam locking system. These systems worked together during the testing to allow for the collection of the necessary data and can be seen in figure 1. In this figure we can see both a photo and a notional diagram of the system assembly. The piezoelectric energy harvester device can be seen as two beam elements in this figure, forming a 'V' shape. The reasons for this design are explained in subsequent sections. The data-logging system consisted of printed circuit board populated with a microcontroller, accelerometer, and memory unit. The tip mass assembly of the beam contained two components necessary to lock and unlock the beam. It contained a wireless receiver, a battery, and a linear servo motor which interacted with the system chassis to lock the beam. The majority of the assembly was surrounded by a 3D printed chassis which provided physical protection for the system, aided in the locking of the harvester assembly, and provided a location to tie the system to the bird. A Rappole-style [15] leg loop harness was used in

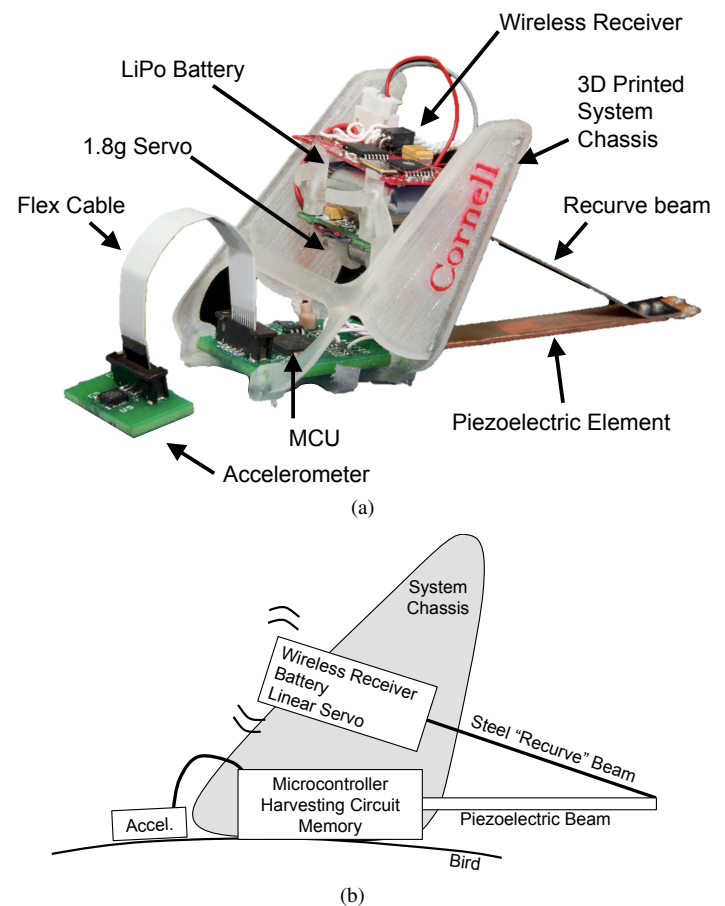


FIGURE 1. (a) Photo of testing system with critical components labeled. (b) Diagram of testing system showing layout of components.

this testing for the main assembly, while the accelerometer board was glued to feathers on the birds back which had been trimmed. Each of these subsystems required significant design and development detailed in the following sections.

2 Piezoelectric energy harvester

The piezoelectric energy harvester beam consisted of a modified Midé Vulture V22BL and an attached recurved stainless steel beam, as shown in figure 2(a). This “recurve” piezoelectric beam configuration is different from the typical simple cantilevered configuration and was originally developed for a similar application on flying moths [8]. The first purpose of the recurve configuration is to allow for reductions in resonant frequency for low mass designs. It is critical that these devices be matched to the excitation frequency for maximum power harvesting. In order to use COTS piezoelectric beam elements, while matching a low excitation frequency of approximately 9 Hz [16] and maintaining a restrictive mass budget, a longer beam must be employed. The recurve configuration effectively increases the length of the beam, which allows for reductions in the resonant frequency of the system for a given mass. Additionally, the configuration allows for changes in the resonances based on the thickness of the recurve section of stainless steel. This makes the system easily reconfigurable to different excitation frequencies. The other reason for the use of a recurve configuration is that it reduces the moment loads at the root of the harvester, as shown in figure 2(b). A typical cantilevered beam would have highest moments at the root of the beam. This moment would act as a pitching torque on the bird in flight. Assuming the mass of the

beam is small compared to the mass at the tip of the beam, the moments applied at the root of a recurved beam would be zero as shown in figure 2(b).

The design of such an energy harvester system for use on a bird requires consideration of the system mass and the excitation frequency target. Using the assumption that the Midé Vulture V22BL beam is uniform across its length, we can predict the entire energy harvesting system natural frequency based on an estimate of the beam stiffness of each section of the recurve system. Using a laser vibrometer, the natural frequency of a clamped Midé Vulture V22BL beam with no tip mass was found on average to be 148.3 Hz when the piezoelectric elements were shorted. Using this, and an estimate of the mass per unit length (12.7 g/cm), we were able to estimate the modulus times the moment of inertia, EI from the following approximation for

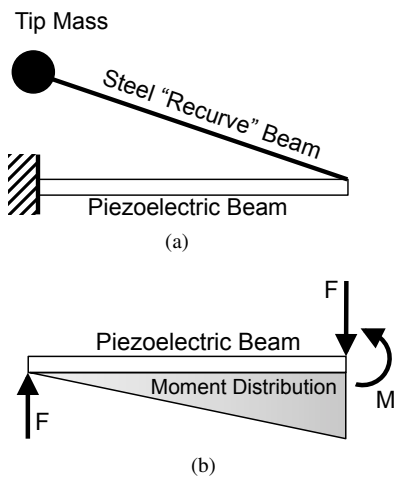


FIGURE 2. (a) Diagram of recurve beam diagram to reduce base moments and decrease natural frequency (b) Approximate free body and moment diagram of piezoelectric beam section of recurve assembly when under load. Notice area of highest bending moment at right side of beam.

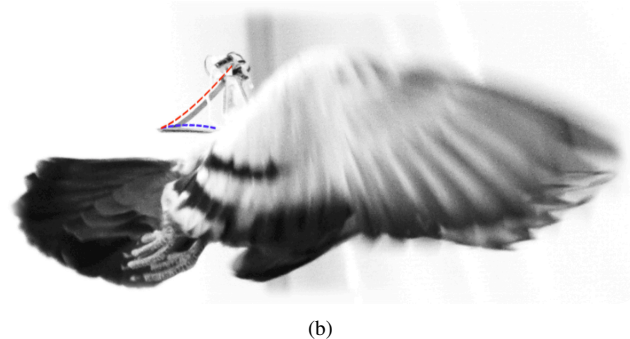
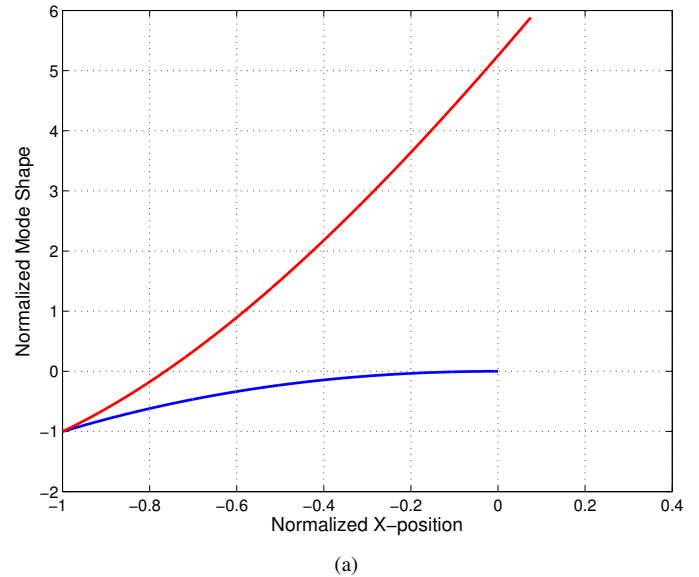


FIGURE 3. (a) Plot of modeshape of recurve piezoelectric energy harvester. Blue line is piezoelectric beam. Red line is stainless steel beam. (b) Modeshape scale and overlaid on beam deflecting in flight.

fundamental frequency of a beam [17]:

$$f = \frac{1.875^2}{2\pi L^2} \left(\frac{EI}{m/L} \right)^{1/2} \quad (1)$$

Solving this expression for EI gives $9.9 \text{ mN}\cdot\text{m}^2$. Knowledge of both this EI parameter and the mass per unit length of the piezoelectric beam allows us to determine the first natural frequency and mode shape of the resulting system. To design this system we used an estimate of the sum of the masses of the components used as the tip mass (4.9 g). Additionally, the EI and mass per unit length parameters for the recurved steel beam section could be calculated directly from the beam's dimension ($57 \times 6.2 \times 0.254 \text{ mm}$). The resulting short circuit natural frequency for the entire recurve piezoelectric energy harvester beam would be 8.5 Hz , near the expected flapping frequency. The mode shape for such a system can be seen in figure 3(a), with the piezoelectric portion of the beam plotted in blue and the stainless steel portion plotted in red. This mode shape can be seen to be excited in figure 3(b), where the modes shape plot has been scaled and overlaid on a photo of one of the birds in flight.

The charge developed by the piezoelectric energy harvesting beam during the flight of the bird was dissipated over a match load resistance. The optimal load resistance for an unrectified low-coupling piezoelectric energy harvester at resonance can be calculated from the following expression [18]:

$$R_{opt} = \frac{1}{C_0 \omega} \quad (2)$$

Here C_0 is the capacitance of the piezoelectric device and ω is the excitation frequency. The capacitance of a Midé V22BL beam with its two piezoelectric elements connected in parallel is 18 nF [19] and we targeted a frequency of 8.5 Hz based on previous measurements of similarly sized birds [16] and the calculated natural frequency of the recurve beam assembly. The result optimal load resistance would thus be $1.05 \text{ M}\Omega$. The optimality of this load resistance was validated in benchtop testing of the system. The resistance used in the final circuit was close to ideal and was $1.110 \text{ M}\Omega$.

The voltage developed by these types of piezoelectric devices are routinely on the order $20\text{-}50\text{V}$, and are thus too high for direct measurements by the microcontroller used by the DAQ system developed for this test. For this reason the circuit shown in figure 4 was used to measure the power dissipated by the load resistance across the piezoelectric elements. The circuit consisted of a voltage divider to reduce the measured voltage to a value within range of the analog-to-digital converter on the microcontroller. Additionally, the measured voltage was biased by half of V_{cc} so to account for the AC nature of the piezoelectric signal.

3 Miniature data acquisition system

The device that monitored the power harvested by the piezoelectric device and the acceleration of the bird was a miniature data acquisition system design specifically for these tests. As seen in the system block diagram of figure 5, this subsystem was centered around an MSP430F2274 microcontroller unit. The microcontroller was programmed to take three measurements at 100 Hz and record the results to a XXXX MByte XXXX flash memory unit. The three measurements that were recorded were the voltage developed over the piezoelectric load resistance, the three axes of acceleration from the Bosch BMA150 accelerometer, and the pulse width modulated (PWM) voltage signal sent to the servo.

The PWM signal was sent from the wireless receiver to the linear servo and controlled the locking and unlocking of the

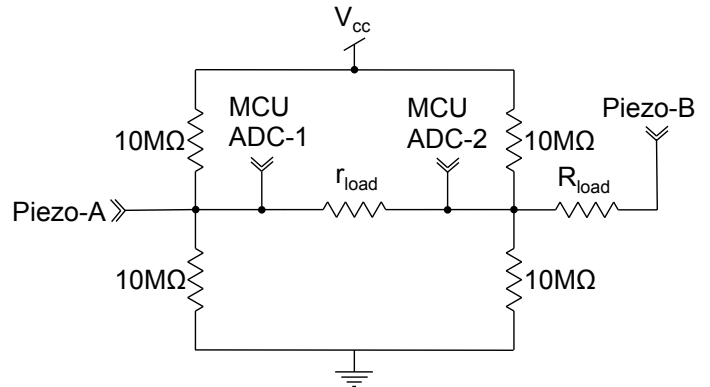


FIGURE 4. Circuit used to read voltage from piezoelectric energy harvester. Voltage divider reduces voltage magnitude to level acceptable to microcontroller and $10\text{M}\Omega$ resistors bias voltage.

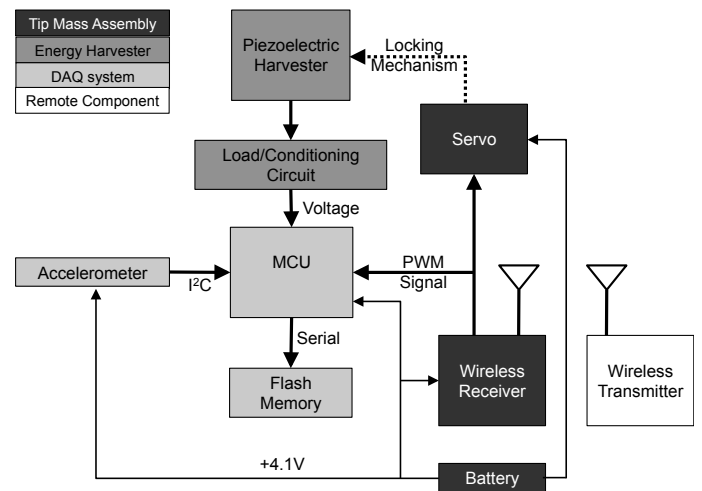


FIGURE 5. Block diagram of mini-DAQ and piezoelectric harvester. Elements in grey were installed as the tip mass of the piezoelectric beam.

piezoelectric device. By taking these three measurements, we were able to understand the dynamics of the bird in flight, the harvested power, and have validation that the harvester was either locked or unlocked for each trial. The PWM signal for the servo control had a typical duration of approximately 1.5 ms, which was below the resolution of the sample record of 100Hz. To account for this, the PWM signal was monitored by an ADC pin on the microcontroller, and a timer with edge detection reset was employed to measure the duration of each pulse. For each recorded datapoint, the MCU logged the most recent pulse duration measured by the timer.

The physical configuration of this system consisted of a printed circuit board that hosted microcontroller and memory modules. This board also served as the physical mount location for the piezoelectric beam. The accelerometer was mounted to a remote board as shown in figure 1 and connected to the main board with a flexible ribbon cable. This was done to minimize any vibrations from the piezoelectric beam being measured by the accelerometer. The power, ground, and PWM connections between the locking assembly on the tip of the beam and the main PCB were made by way of a braided bundle of flexible 36 AWG silicone coated multi-strand wires.

4 Energy harvester locking mechanism

The locking mechanism used in this system to arrest the motion of the harvester during flight can be seen in figure 6. The mechanism that locked the beam was integrated as part of the tip mass of the recurve beam. The locking device consisted of a battery (Plantraco FR-30 bare cell lithium polymer, 1 g), a wireless receiver (Plantraco Micro9-S-4CH, 1.1g), and a linear servo motor (Spektrum SPMSA2005, 1.8g). A chassis for mounting this hardware was printed using a Objet Connex500 3D printer using Fullcure720 resin. The operation of the mechanism was initiated by operating one of the controls of the wireless transmitter paired to the wireless receiver. When signaled, the receiver would change the duty cycle of the PWM signal sent to the linear servo mechanism. The servo in response would change position, moving the pushrod (shown in figure 6) in or out. When the rod was moved out it would contact the system chassis shown in figure 1(a). The force applied to the pushrod by the servo would then wedge the tip mass assembly between the vertical "wings" of the system chassis, effectively locking the tip mass assembly in place.

The general operation of the DAQ system, the energy harvester, and the locking tip mass assembly can be seen in the testing result shown in figure 7. This plot show the typical result of the testing, demonstrating the locking and unlocking of the energy harvesting beam element. In this figure, we see three subplots including the z-component of acceleration, the output of the PWM beam locking signal, and the voltage developed by the energy harvesting element. These three signals are all plotted

against time. We can see in this figure that the tip mass is initially locked. The four discrete instances of z-acceleration shown in the first plot of this figure are individual flights of the bird as it flew between perches. We can see that the bird made two flights between perches before the tip mass assembly was unlocked. During the lock flights, the third plot shows almost no voltage was developed by the energy harvester, demonstrating that the beam was effectively locked in place and not vibrating. At approximately $t = 145$ s, while the bird was perched, the tip mass assembly was unlocked. The bird was then prompted to make two more flights with the vibrating energy harvester attached. During these two flight, voltage was developed across the harvester load resistance, indicating that power was harvested.

5 Testing Results

Testing of these energy harvesting devices were conducted on three birds and resulted in 69 flights with the beam energy harvester device locked in place and 67 flights with the system unlocked and harvesting power. The device can be seen mounted to the 589 g male pigeon in figure 8. The 11.9 g testing device thus represented 2% of the mass of the bird, below the 3-5% limit discussed in literature [11] [12] [13] [14]. In this photo, the mounting location and size of the system can be seen with respect to the bird. The flexible ribbon cable connecting the main PCB to the accelerometer can be seen, and shows the approximate location of the accelerometer on the bird as well.

An example of the acceleration profile that was recorded for one of the unlocked system flights can be seen in figure 9. In

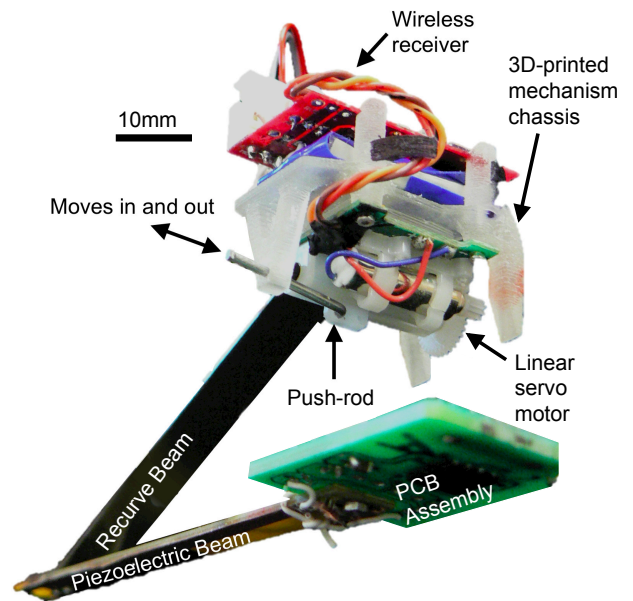


FIGURE 6. Photo of system without system chassis and accelerometer. Shown to highlight locking mechanism.

this figure, three graphs are shown, one for each component of acceleration using a coordinate system fixed the the bird. The x-direction was in the forward direction of flight, the y-direction was toward the bird's left wing, and the z-direction pointed up off of the bird's back. The data presented here as been high-pass filtered to remove the DC component of acceleration related to gravity. In this plot we see the highest accelerations at the beginning and ends for the flight when the bird is taking off and landing. The acceleration peaks in the z-direction were nearly 4g's and 3 g's in the x-direction. This shows that while an energy harvesting beam could be mounted in the z-direction to harvest energy from the x-component of acceleration, the z-direction has higher acceleration magnitudes and would produce more power. Furthermore, this orientation would produce less drag on the bird than a beam mounted in the z-direction. In this figure we see very little acceleration in the y-direction. This is to be expected as the birds were flying in straight lines between perches. The mean fundamental frequency for this flight was 7.5 Hz, which while less than the targeted 8.5 Hz for the energy harvesting system was close enough to induce a significant response in the energy harvesting system.

The voltage, instantaneous power, and sliding windowed RMS power developed by the piezoelectric energy harvester over the flight shown in figure 9 can be seen in figure 10. In the first graph of this figure we see a voltage developed by the piezoelectric device matching the the z-component acceleration profile, with high initial and final amplitudes. The voltage amplitude varied between approximately 9 and 25 V for this trial and was similar in other trials. The instantaneous power developed over the 1.11 MΩ load resistance can be seen in the second graph of

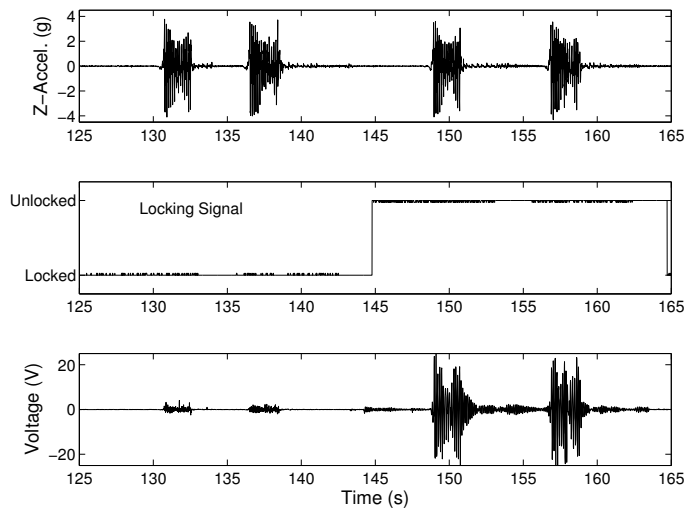


FIGURE 7. Acceleration, locking signal, and harvester voltage vs. time showing near zero harvester voltage when locked down despite motion of bird.

figure 10. In this plot, we see instantaneous power peaks reaching as high as 0.72 mW during the landing and closer to 0.2 mW during the central portion of the flight. In the third graph of this figure, we present a sliding window RMS result. The window size used was 0.54 s, representing approximately 5 flapping cycles of the bird. This result gives a better estimate of what the harvester would produce if the signal were rectified and used to power a circuit or charge a battery. We can see that in this graph that the RMS power varies between 0.075 mW and 0.22 mW.

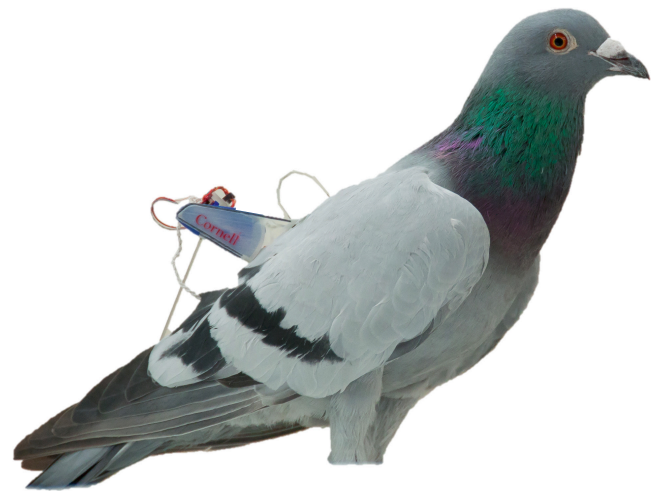


FIGURE 8. System mounted to back of pigeon

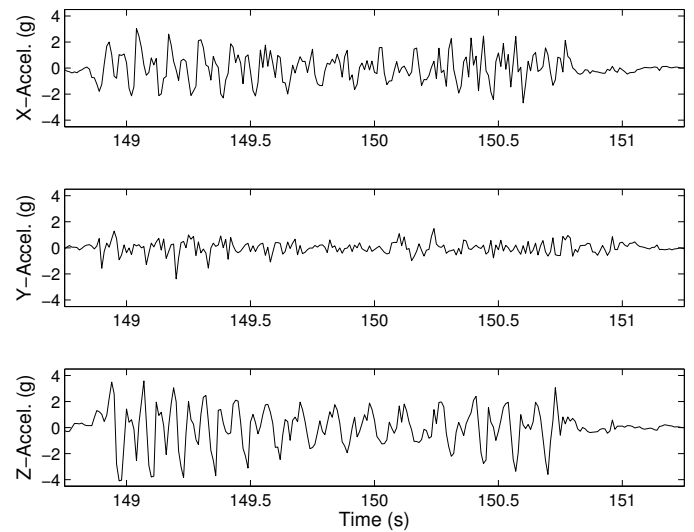


FIGURE 9. Plots of three acceleration components for typical flight.

6 Discussion

This work has demonstrated the feasibility of harvesting energy using piezoelectric devices on flying birds. We have developed a system that is capable of harvesting the energy generated in the piezoelectric device and is capable of measuring the accelerations of the birds in flight at the same time. While the detailed analysis of the flights comparing the acceleration of the birds with and without the vibrating system is ongoing, we have shown the functionality of the system here and shown some initial acceleration and power results.

The RMS power that was developed in flight was on the order of 0.1mW. This amount of power is significant considering two facts. The piezoelectric element employed was a modified off the shelf component. These devices are not optimized for power production, and we could expect more power if a piezoelectric device were optimized and fabricated specifically for the mass and frequency targets of the bird under testing. Other work has shown that the piezoelectric material thickness and aspect ratio of these harvesters are critical design considerations when developing systems for fixed mass, frequency, and excitation acceleration constraints [20] [21]. Despite this fact, the amount of power harvested was still capable of powering a microcontroller-based circuit. An RMS power on the order of 0.1mW is significant given the power requirements of the modern microcontrollers that would be used to run bio-logging devices. There are a significant number of devices on the market, but many contain features not necessary for a bio-logging device. Table 1 provides basic power requirements of some low-power devices that could be used on an avian bio-logger. In this table we see that the power consumption of these devices is on the order of hun-

TABLE 1. Power consumption for example microcontroller devices

Manufacturer	Model	Power@1MHz (mW)
Texas Instruments	MSP430F2XX	0.44
	MSP430FR5X	0.18
Atmel Corporation	ATtinyX4A	0.38
	ATtinyX61/V	0.54
	ATmega165	0.39

dreds of microwatts. These power values could be significantly reduced by reductions in the clock frequency of the microcontroller, as the current draw of these devices is linearly related to the clock frequency. Regardless of reductions to the clock frequency, comparing the power required to run a microcontroller with the 0.1mW produced by the piezoelectric energy harvester in flight shows that these energy harvesters produce power on an order of the power requirements of the microcontrollers used in bio-logging applications. Furthermore, these bio-logging devices are typically duty cycle managed and only spend a short portion of the day in active mode. For reference the low-power “sleep” mode of the microcontrollers listed in table 1 is on average 190nW, or approximately three orders of magnitude less than what was produced in testing. This further shows that there is sufficient power produced by these piezoelectric energy harvesters to warrant their use on bio-logging devices.

Acknowledgements

This research was supported by NSF grant No. CMMI-1014891 and the NSF Graduate Research Fellowship Program.

REFERENCES

- [1] Naito, Y., 2004. “New steps in bio-logging science”. *Mem Natl Inst Polar Res Spec*(58), pp. 50–57.
- [2] Scholander, P. F., 1940. “Experimental investigations on the respiratory function in diving mammals and birds”.
- [3] Kooyman, G. L., 1965. “Techniques used in measuring diving capacities of weddell seals”. *Polar Rec*, **12**(79), pp. 391–394.
- [4] Kooyman, G. L., 2004. “Genesis and evolution of bio-logging devices: 1963–2002”. *Mem. Natl Inst. Polar Res.*, **58**, pp. 15–22.
- [5] Ropert-Coudert, Y., and Wilson, R., 2005. “Trends and perspectives in animal-attached remote sensing”. *Frontiers in Ecology and the Environment*, **3**, pp. 437–444.
- [6] Jouventin, P., and Weimerskirch, H., 1990. “Satellite tracking of wandering albatrosses”. *Nature*, **343**, pp. 746–748.

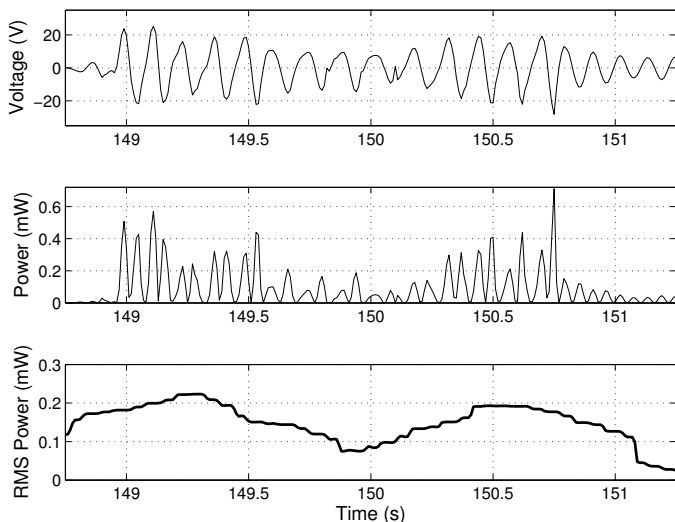


FIGURE 10. Plot of voltage over load resistance, power dissipated by load resistance, and RMS of dissipated power. RMS calculation uses a 0.54 s sliding window.

- [7] Burgess, W., Tyack, P., Le Boeuf, B., and Costa, D., 1998. “A programmable acoustic recording tag and first results from free-ranging northern elephant seals”. *Deep-Sea Research Part II*, **45**(7), pp. 1327–1351.
- [8] Reissman, T., MacCurdy, R. B., and Garcia, E., 2011. “Electrical power generation from insect flight”. *Proc. SPIE 7977, Active and Passive Smart Structures and Integrated Systems 2011*, **7977**, April, pp. 797702–797702–9.
- [9] Aktakka, E. E., Kim, H., and Najafi, K., 2011. “Energy scavenging from insect flight”. *J. Micromech. Microeng.*, **21**(095016).
- [10] Shafer, M. W., and Garcia, E., 2011. “Maximum and practical sustainably harvestable vibrational power from avian subjects”. *ASME 2011 Conference on Smart Materials, Adaptive Structures and Intelligent Systems (SMASIS2011)*, **2011**(54723), pp. 353–359.
- [11] Naef-Daenzer, B., Widmer, F., and Nuber, M., 2001. “A test for effects of radio-tagging on survival and movements of small birds”. *Avian Science*, **1**(1), pp. 15–23.
- [12] USGS, 2011. How to request auxiliary marking permission. <http://www.pwrc.usgs.gov/bbl/manual/aarequs.cfm>. [Online; accessed February 28, 2012].
- [13] Hill, D., and Robertson, P., 1987. “The role of radio-telemetry in the study of galliformes”. *World Pheas. Assoc. J.*, **12**, pp. 81–92.
- [14] Hedin, R., and Caccamise, D., 1982. “A method for selecting transmitter weights based on energetic cost of flight”. In *Trans Northeast Fish Wildl Conf*, Vol. 39, p. 115.
- [15] Rappole, J. H., and Tipton, A. R., 1991. “New harness design for attachment of radio transmitters to small passerines”. *Journal of Field Ornithology*, **62**(3), pp. 335–337.
- [16] Tobalske, B. W., Hedrick, T., and Biewener, A. A., 2003. “Wing kinematics of avian flight across speeds”. *Journal of Avian Biology*, **34**, pp. 177–184.
- [17] Blevins, R. D., 1979. *Formulas for Natural Frequency and Mode Shape*. Krieger Publishing Company.
- [18] Guyomar, D., Badel, A., Lefeuvre, E., and Richard, C., 2005. “Toward energy harvesting using active materials and conversion improvement by nonlinear processing”. *IEEE Transactions on Ultrasonics, Ferroelectrics, and Frequency Control*, **52**(4), April, pp. 584–595.
- [19] Midé, 2013. Vulture piezoelectric energy harvesters datasheet, January.
- [20] Shafer, M. W., Bryant, M., and Garcia, E., 2012. “Designing maximum power output into piezoelectric energy harvesters”. *Smart Materials and Structures*, **21**(8).
- [21] Shafer, M., and Garcia, E. “The power and efficiency limits of piezoelectric energy harvesting”. *Journal of Vibrations and Acoustics*, (*in review*).